Turkish Journal of Chemistry

Volume 44 | Number 4 Article 18

1-1-2020

New sandwich-type polymeric potassium-dicyanoargentate(I) complex: synthesis, characterization and enzymatic activity

NESRİN KORKMAZ

TÜBİTAK

Turkish Journal of Chemistry

http://journals.tubitak.gov.tr/chem/

Research Article

Turk J Chem
(2020) 44: 1110 – 1121
© TÜBİTAK
doi:10.3906/kim-2004-42

New sandwich-type polymeric potassium-dicyanoargentate(I) complex: synthesis, characterization and enzymatic activity

Nesrin KORKMAZ*
Department of Biotechnology, Faculty of Science, Bartın University, Bartın, Turkey

Received: 12.04.2020 • **Accepted/Published Online:** 15.06.2020 • **Final Version:** 18.08.2020

Abstract: Coordination compounds containing dicyanoargentate(I) have remarkable biological potential due to their therapeutic antibacterial, antifungal, antibiofilm, and anticancer properties. In this study, a new dicyanoargentate(I)-based complex was synthesized and characterized by various procedures (elemental, thermal, FT-IR for complex) involving crystal analysis of the complex. In addition, the biological activity of this new compound on the acetylcholinesterase (AChE) enzyme, an important enzyme for the nervous system, was investigated. When the infrared (IR) spectrum of the complex is examined, the OH vibration peak resulting from H_2O molecules in the structure at 3948-3337 cm^{-1} and at 2138 cm^{-1}, along with a CN peak coordinated to Ag, can be seen, indicating that the mass remaining in the thermal degradation of the complex at 1000 °C is the weight corresponding to the metal mixture consisting of K + Ag (calc.: 68.06). The crystal method revealed that the complex has a sandwich-like, polymeric chemical structure with layers formed by K^+ cations and $[Ag(CN)_2H_2O]^-$ anions. Therefore, the AChE enzyme has potential therapeutic uses in improving ACh levels in brain cells, in reducing various side effects, and in improving cognitive impairment, especially in advanced Alzheimer's disease patients. In this study, the activity of this newly synthesized complex on AChE was also investigated. As a result of this research, $[Ag(CN)_2(H_2O)K]$ had 0.0282 ± 0.010 μM Ki values against AChE. The compound was therefore a good inhibitor for the AChE enzyme. This type of compound can be used for the development of novel anticholinesterase drugs.

Key words: Silver complexes, X-Ray, metabolic enzymes, enzyme inhibition, acetylcholinesterase

1. Introduction

Coordination polymers are compounds obtained by the linking of metal atoms with bridge ligands in an infinite arrangement [1]. The choice of the ligand used in the synthesis of coordination polymers is of great importance because coordination polymers have different structures and properties depending on the ligands they contain. The most important feature of the ligands used for this purpose is the ability to bridge the metal centers. Therefore, these ligand molecules should be multident ligands having two or more donor atoms and which generally contain groups such as N-, O-, S-, or CN-, which have high donor properties. Examples of these bridge ligands are SCN-, CO, N_3^-, NCX^- (X: O, Se, S), I_2, NO_3^-, and CN^- ligands. These ligands are preferred because they can exhibit ambidentate properties and are extensively used in the synthesis of coordination compounds [2,3].

In recent years, a number of cyanido complexes have been characterized by synthesizing a wide variety of transition metals and cyanido ligands. In several comprehensive studies, $[M(CN)_4]^{2-}$ (M^{II} = Ni, Pd, Pt, Ag,

*Correspondence: nkorkmaz@bartin.edu.tr

and Au) anions, Ni^{II}, Cu^{II}, Zn^{II}, and Cd^{II} secondary metal ions, as well as a series of bimetallic cyanido containing auxiliary ligands with N and O donor atoms, have been used by researchers to synthesize the complex. The structural characterizations of these complexes, catalysis applications, EPR properties of the d^9 structure, as well as biological properties, have been determined [4–16].

Silver compounds have been the subject of many studies attracting the attention of scientists because of their many useful properties. When examined in terms of electron distribution, Ag^+ ion, which is a d^{10} structure, can produce interesting coordination geometry with different supramolecular and molecular structures [17–22]. Since ancient times, experimenting with and using the biological activity of silver has led to more and more experiments and studies. The antibiotic effect of silver compared to conventional antibiotics has been reported to be more effective in various studies [23,24]. Therefore, it may be an alternative for bacteria with high antibiotic resistance [25,26]. Silver not only intitiates activity against bacteria but also affects nanoparticles through antibiofilm action; compounds containing silver that exhibited antitumor activity have also been reported in the literature [27–32]. Furthermore, Ag^I compounds have different applications as catalysts in organic synthesis reactions [32,33]. The antibacterial, antibiofilm, antifungal, and anticancer properties of dicyanidosilver(I) complexes have been investigated recently and their potential to be antiagents due to their very good biological activity has been observed [12–14,30–32]. These substances are synthesized quickly, easily, and with high efficiency, so their low cytotoxicity is of great importance for biological studies.

In this study, heteroleptic cyanidoargentate, i.e. the $[Ag(CN)_2(H_2O)K]$ complex to which the CN^- and H_2O ligands are linked, has been successfully synthesized (Scheme). This novel heteroleptic complex was characterized by elemental analysis, FT-IR, thermal analysis, and X-ray single crystal analysis. In addition, the inhibition activities of $[Ag(CN)_2(H_2O)K]$ complex against acetylcholinesterase (AChE) metabolic enzyme were obtained in this study.

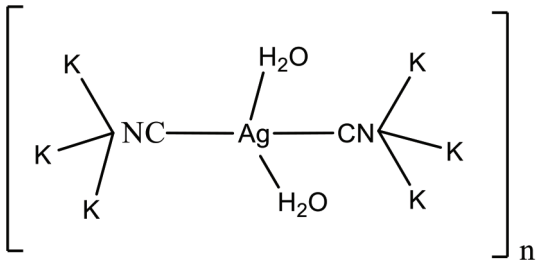

Scheme. Complex consisting of a reaction of silver nitrate and potassium cyanide.

2. Experimental section

2.1. Synthesis and characterization

The synthesis was carried out in a water bath at 40 °C for 4 days. The KCN (153 mg, 1.175 mmol) was dissolved in 20 mL of purified water. The previously dissolved water solution of KCN was added to $AgNO_3$ solution (200 mg, 1.177 mmol) and dissolved in a mixture of ethanol (10 mL) and water (20 mL). The clear $K[Ag(CN)_2]$ solution was then stirred for 4 h. The product was filtered and allowed to crystallize in a 40 °C water bath. $[Ag(CN)_2(H_2O)K]$ crystals were obtained at a high yield 4 days later (yield: 79%). Elemental analysis of the sample was taken according to the standard (C, N, H, and O values) method. The IR spectrum of the sample

was taken as powder in the Shimadzu IRAffinity-1 spectrophotometer in the range of 4000–400 cm^{-1}. Thermal degradation of the obtained complex was performed with a Hitachi STA 7300 TG/DTG thermal analyzer and analyzed at 5 °C/min using a platinum crucible under nitrogen atmosphere at a heating speed in the 25–1000 °C temperature range. X-ray single-crystal analysis was performed on a Bruker APEX-II CCD detector. The crystal data and test conditions of the complex are presented in Table 1.

Table 1. Crystallographic data and structure parameters for the $[Ag(CN)_2(H_2O)K]$ complex.

Empirical formula	$C_2H_2AgKN_2O$
Formula weight	217.03
Temperature [K]	296
Crystal size [mm]	0.11× 0.08 × 0.07
Crystal system	Trigonal
Space group	$P3_1/c$
a [Å]	7.3867 (13)
b [Å]	7.3867 (13)
c [Å]	17.598 (4)
$\alpha = \beta$ [°]	90.00
γ [°]	120
V [$Å^3$]	831.6 (3)
Z	6
ρcalcd. [g/cm^3]	2.588
μ [1/mm]	4.26
F(000)	606
θ range [°]	3.2–26.4
Index ranges	±9, ±9, ±22
Reflections collected	3416
Reflections observed (>2σ)	525
Data/restrains/parameters	574/3/38
R1 (all)	0.052
wR2 CCDC No.	0.185 1958042
Kristolografi doi	10.5517/ccdc.csd.cc23qhn0

2.2. Inhibition studies of acetylcholinesterase

The inhibition potency of $[Ag(CN)_2(H_2O)K]$ novel complex on AChE activity was measured using Ellman's procedure (1961) with spectrophotometrically [34]. Acetylthiocholine iodide (AChI) was used as a substrate of the enzymatic reactions and 5,5' -dithio-bis(2-nitro-benzoic)acid (DTNB) for the estimation of the AChE activities. The reaction mixture consists of 100 mM Tris-HCI (pH = 8), 10 mM AChI, 10 mM DTNB, 15 μL AChE solution, and different concentrations of sample complexes. The absorbance change of the mixture was read at a wavelength of 412 nm.

3. Results and discussion

3.1. Elemental analysis

Elemental analysis data were found as follows; Anal. Calc. (%) for C_2HN_2OAgK: C, 11.12%; H, 0.47%; N, 12.97%; O, 7.41; found: C, 12.08%; H, 0.82%; N, 13.69%; O, 6.96%.

3.2. IR spectra

IR spectroscopy is a method used to characterize organic or inorganic compounds. The IR spectrum shows, for example, the fingerprint with absorption peaks corresponding to the frequencies generated by the vibration of the bonds between the atoms forming the substance. Each substance has its own spectrum [35,36]. The most characteristic and distinctive peak in this cyanido complex is the vibration peak of the cyanido group. It is known that free cyanide gives $\upsilon(C\equiv N)$ vibration peak at 2080 cm^{-1}. When the CN^- group coordinates to a metal, it gives electrons to the metal with the donor character σ and accepts electrons again by binding (π-receptivity). Since the electron pair introduced to the metal moves away from the σ orbital of the nonbonding (slightly weaker opposing bond character) carbon, the σ-transmittance $\upsilon(CN)$ while the electrons coming back by binding are located in the orbital molecule π^*, the π-back binding causes $\upsilon(CN)$ to fall. Since the σ-donor character of the CN group is more dominant than the π-acceptor character, it shifts to higher frequencies in coordinated cyanido groups. In addition, depending on the electronegativity of the metal, the oxidation step and the number of coordinations of the vibration frequency $\upsilon(C\equiv N)$ shifts to a higher area. If both bridges and end cyanido groups are present in the structure, $\upsilon(CN)$ is split in half. The cyanido group, which has a higher wavenumber than the peaks, belongs to the cyanido group, while the cyanido groups that do not participate in the bridge formation are observed at a lower wavenumber [37].

In light of this information, the stretching vibration of the CN peak, which shows chelate, is seen as a sharp peak at 2086 cm^{-1} (Figure 1). The peaks seen in the 1400–1600 cm^{-1} range are thought to belong to the bending vibrations of the CN group.

When the IR spectrum of the complex in Figure 2 is examined, the OH vibration peaks at 3288 cm^{-1} and at 2137 cm^{-1} the CN peak coordinated to the metal can be seen. The peaks seen in the 1400–1600 cm^{-1} range are thought to belong to the bending vibrations of the CN group. In addition, the peaks at 600–400 cm^{-1} are thought to be related to the υ(Ag-C), υ(K-N), and υ(Ag-O) vibrations. The presence of this peak in the spectrum and free cyanide observed in our complex shows the formation of shear.

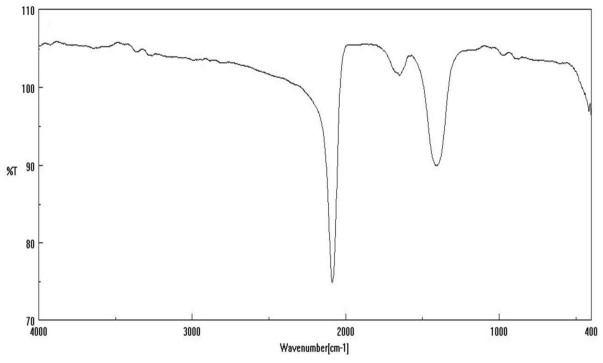

Figure 1. IR spectrum of KCN.

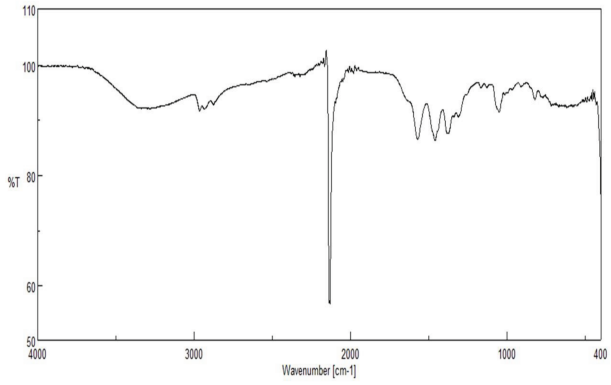

Figure 2. IR spectrum of the complex.

3.3. Thermal analyses

Thermal analysis is a method by which certain physical changes in the sample are recorded as a function of temperature or time when heating or cooling according to a predetermined schedule. Thermogravimetric/thermogravimetric derivative–differential thermal analysis (TG/DTG − DTA) measurements of the complex also support the crystal composition as shown in Figure 3.

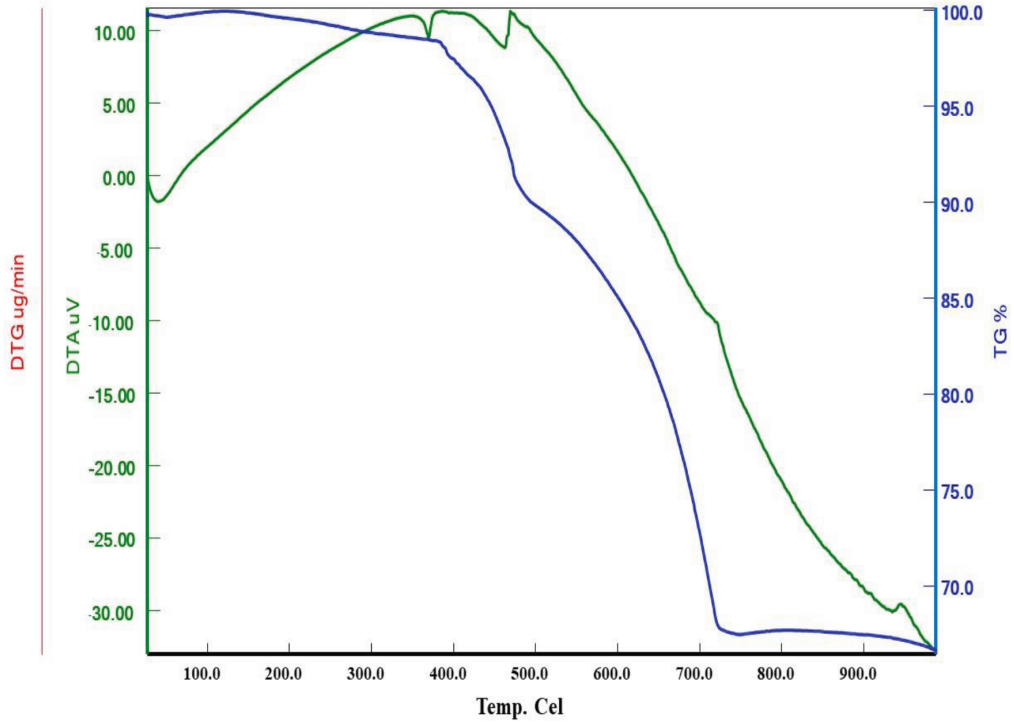

Figure 3. Thermal analyses curves of complex.

The TG/DTG curves of the complex are followed by a process in which a two-step weight loss is observed from 30 °C to 1000 °C. The sharp peak at 160–480 °C in the thermal decomposition graph of complex corresponds to an H_2O ligand. The H_2O molecule is attached to the silver atom by a σ bond. Therefore, the bond breaks down, and the decomposition of the water molecule also takes place at higher temperatures. The H_2O ligand is degraded in the initial steps of the thermal decomposition, which is followed by the thermal degradation of the cyanido ligand. Finally, the final stage of the thermal decomposition is the temperature at which the inorganic components corresponding to the metal residues are located. Experimental data indicate that the mass remaining in the thermal degradation of the complex at 1000 °C is the weight corresponding to the metal mixture consisting of K + Ag (calc.: 68.06; found: 67.9).

3.4. Crystal structure of complex

X-ray crystallography is used to determine the atomic or molecular structure of a crystal. Since salts, metals, minerals, semiconductors, as well as various inorganic, organic and biological molecules can form crystals, X-ray crystallography is important in many scientific fields. The structure of the substance we obtained in our study was illuminated by X-ray crystallography. During single crystal analysis, a heterobimetallic complex (K-Ag) appeared. In addition to the CN ligand in the structure, it formed a heteroleptic dicyanidoargentate complex

by binding to Ag(I) as a ligand in the water molecule. The CN ligand acts as a bridge between the Ag and K atoms. Crystal structure analysis reveals that the complex is formed by $[Ag(CN)_2(H_2O)K]$ units (Figure 4). Ag(I) was coordinated with 2 C atoms of bridging cyanido ligands and the O atom of 2 water molecules.

Potassium atoms are connected together in the form of cubes intertwined by the binding of N atoms above and below the plane (Figure 5). Here, the K atoms exhibited a structure similar to the 6 coordinated K complexes in the literature [38–40].

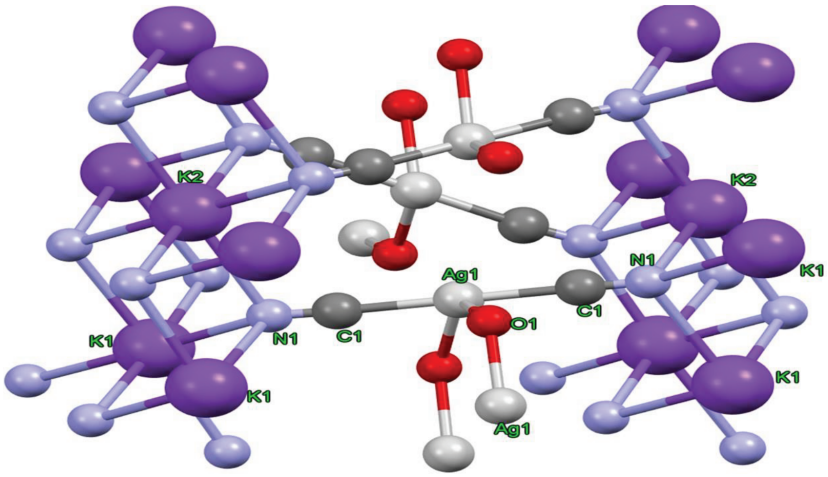

Figure 4. Crystal structure of $[Ag(CN)_2(H_2O)K]$ as obtained by low temperature X-ray crystallography.

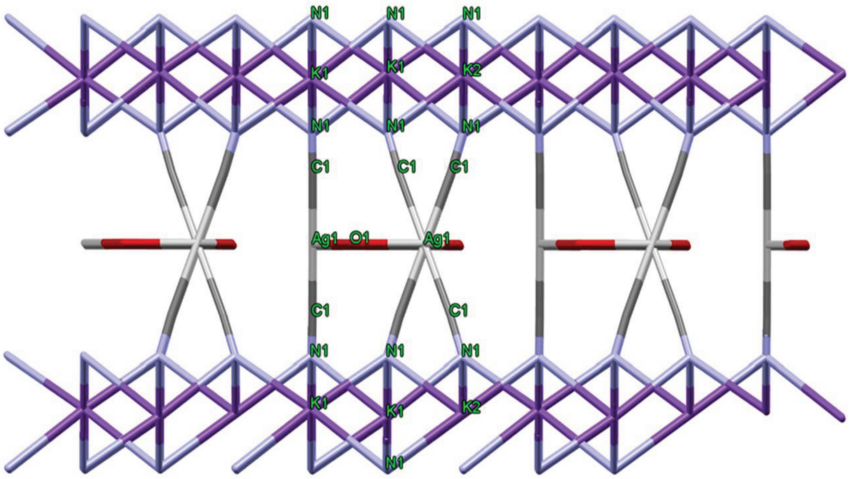

Figure 5. Sandwich-type topology of the complex.

Again, the K atoms above and below the plane are connected to each other by $Ag(CN)_2$ bridges (sandwich-like). Between the K layers, hexagonal intermediate structures consisting of 3Ag + 3O made interesting contributions to the stacking of the complex (Figure 6). The K-N bond distance with 6 coordinated octahedral geometry ranges from about 2.80 to 2.90 Å (Table 2). The angles between N1-K1-N1 and N1-K2-N1 vary between 83.9 (3) and 96.2 (2).

Although the geometry around Ag(I) is a linear structure formed by the linkage of the bridge CN groups, a geometry near the "T shape" emerges as a result of the binding of H_2O molecules.

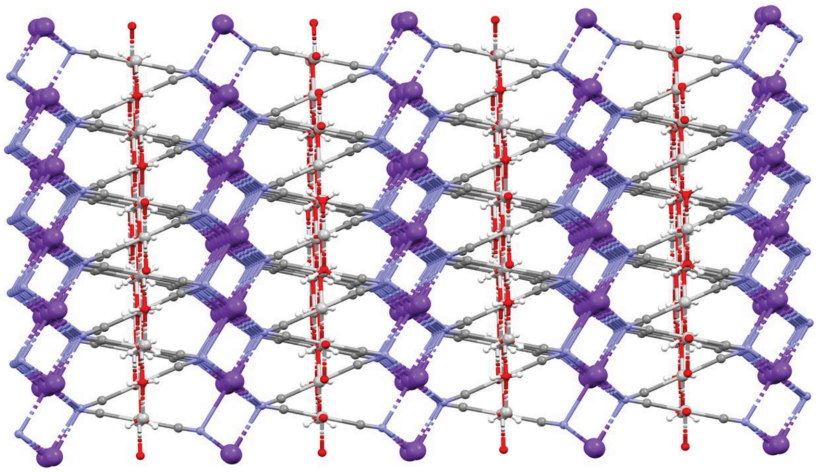

Figure 6. 3D configuration view of the complex.

Table 2. Selected bond lengths [Å] and angles [°] for complex.

Bond lengths			
Ag1-C1	2.054(10)	C1-K1^{i}	3.468 (11)
Ag1-O1	2.070(11)	K1-N1^{iv}	2.823 (9)
K1-N1	2.824(9)	K1-N1^{i}	2.906 (9)
K2-N1	2.868(8)	O1-H1	0.84 (2)
Ag1-C1^{ii}	2.054(10)	N1-K1^{i}	2.906 (9)
Ag1-O1^{iii}	2.070(11)	K1-N1^{v}	2.823 (9)
Bond angles			
N1-C1-Ag1	175.6(10)	N1^{vii}-K1-K2	42.05 (16)
N1-C1-K2	51.8(6)	N1^{i}-K1-K2	89.35 (17)
Ag1-C1-K2	125.0(5)	C1^{i}-K1-K2	94.4 (2)
N1-C1-K1^{i}	51.7(7)	C1^{vii}-K1-K2	51.32 (17)
Ag1-C1-K1^{i}	126.0(4)	C1^{vi}-K1-K2	119.9 (2)
K2-C1-K1^{i}	76.5(2)	K2^{viii}-K1-K2	119.953 (4)
C1^{ii}-Ag1-C1	179.8(6)	N1-K2-N1^{vi}	83.8 (2)
C1^{ii}-Ag1-O1	110.5(3)	N1^{xii}-K2-N1	96.2 (2)
O1-Ag1-O1^{iii}	116.2(11)	C1-K2-C1^{xi}	71.6 (3)
C1-N1-K1	139.0(9)	N1^{iv}-K1-N1^{v}	98.4 (2)
C1-N1-K2	110.1(8)	N1^{iv}-K1-N1^{vi}	83.9 (3)
K1-N1-K1^{i}	96.3(2)	N1-K1-C1^{i}	98.8 (3)
K2-N1-K1^{i}	95.2(3)	N1^{v}-K1-C1^{vi}	159.1 (3)

Symmetry codes: (i) −x+1, −y+1, −z+1; (ii) −x+y, y, −z+1/2;
(iii) −x+y, −x+1, z; (iv) −y+1, x−y, z; (v) −x+y+1, −x+1, z;
(vi) x−y+1, x, −z+1; (vii) y, −x+y, −z+1; (viii) x+1, y, z;
(ix) x+1, y+1, z; (x) x−y, x, −z+1; (xi) −x+y, −x, z; (xii) −y, x−y, z;
(xiii) −x, −y, −z+1; (xiv) −y+1, x−y+1, z.

The deviation in T geometry was impaired by the small angle at 69.7(3)°, which is thought to be caused by steric repulsion and H-bond formation between water molecules (Table 2). The Ag-C bond length of the complex (2.054 Å) is similar to those of dicyanidoargentate(I) complexes observed in the literature [12,30,31].

Intermolecular interaction analysis shows that cyanide N atoms occur between H atoms of the water molecules (Table 3). The formation of the H-bond contributes to better packaging of the structure by providing extra stability to the structure.

Table 3. Selected intermolecular distances [Å] and angles [°] of C3.

D−H···A	d(D–H)	d(H···A)	d(D···A)	D–H···A
O1–H1..···N1^{xv}	0.84 (2)	2.60 (3)	3.182 (8)	128 (4)

Symmetry code: (xv) $-y+1$, $-x+1$, $-z+1/2$.

3.5. AChE enzyme results

AChE is found in the brain and in erythrocytes at high concentrations, and it is a crucial enzyme for the nervous system. AChE inhibitors are used in the treatment of several neuromuscular diseases and in the treatment of AD [41]. The half-maximal inhibitory concentration (IC_{50}) values of the novel compound demonstrated 50% inhibition of AChE calculated after suitable dilutions. The Ki value of the new compound was determined for AChE. Ki is defined as the binding affinity constant of the novel compound to AChE. To demonstrate the nonallosteric nature of the enzymatic reaction, an enzymatic activity curve (Michaelis–Menten) was first generated. After Vmax stabilization, Lineweaver–Burk graphic studies were performed using inhibitory concentrations of the complex. To determine the Ki values, the novel compound was tested at 3 different concentrations. Michaelis–Menten and Lineweaver–Burk curves were drawn in detail as described previously [41,42]. For descriptions of inhibitory effects, researchers have often used an IC_{50} value; however, the Ki constant is a more suitable parameter. Ki values were calculated from Lineweaver–Burk graphs (Figures 7 and 8). The novel complex exhibited inhibitory effects on AChE, and the inhibition effect is shown in Figure 6. The Ki constant of AChE was found to be 0.0282 ± 0.010 mM, and IC_{50} values of the compound against AChE were noted as 1.32 mM (r^2: 0.99). In addition, tacrine (TAC) was used as positive control AChE inhibitor, and it had Ki values corresponding to 392.18 ± 66.28 μM. The IC_{50} values of these natural compounds and standard (tacrine) showed the following order: TAC (409.10 μM, r2: 0.9601) < compound (1.32 mM, (r2: 0.99)) for AChE (Table 4). The inhibition type of the complex is competitive against AChE enzyme activity because, while looking at the inhibition mechanism in the presence of the complex, it is possible to say that it shows a competitive inhibition mode from the specific rate graph. Acetylcholinesterase inhibitors (AChEIs) like TAC are commonly used in therapies related to Alzheimer's disease [43]. Recently, the biological activity of various molecules and metal complexes has been investigated, and research efforts have focused on developing new candidate complexes to investigate their biological potency. As a result, it has been reported that the novel complex worked for the first time, and it has an in vitro inhibitory effect on the AChE enzyme. The inhibitory effect of this molecule on other enzymes should therefore be investigated in different studies.

4. Conclusion

In summary, the $[Ag(CN)_2(H_2O)K]$ complex, consisting of linear CN groups of Ag cations with an electronic configuration of $4d^{10}$, was synthesized and characterized. X-ray spectra exhibited an interesting 3D, sandwich-like structure by hexagonal $[Ag(H_2O)]$ clusters connecting the infinite $[K(CN)_2]$ layers of the complex. It was observed from complex TG analysis that it showed a two-step degradation between 30 and 1000 °C. The H_2O ligand is disrupted in the early stages of thermal decomposition, followed by thermal disruption of the cyanido ligand. After thermal decomposition, a residue corresponding to the Ag + K metal mixture remained in the

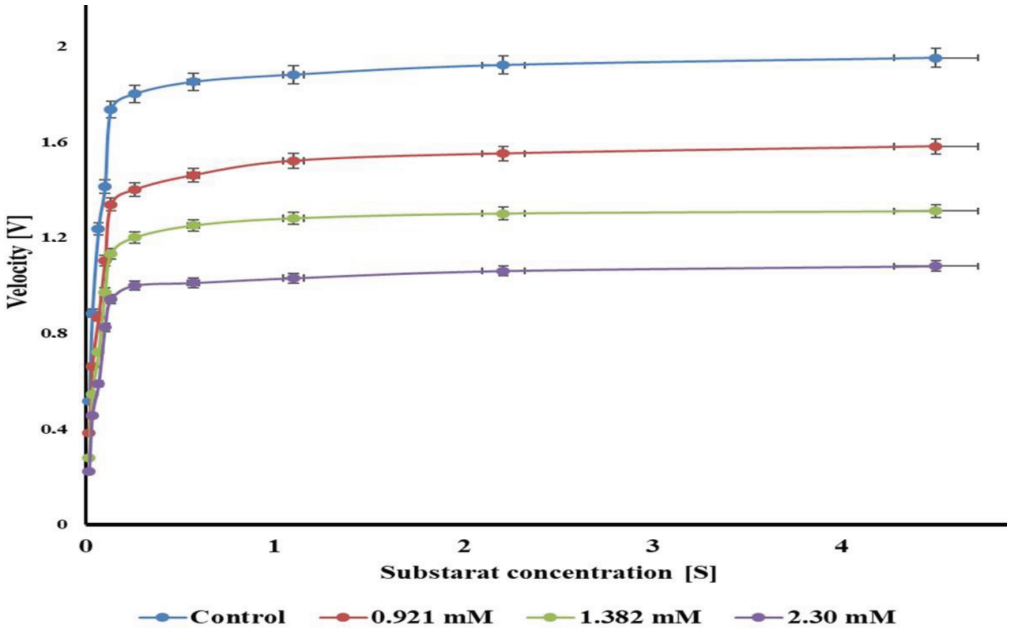

Figure 7. Effect of $[Ag(CN)_2(H_2O)K]$ on AChE enzyme inhibition (Michaelis–Menten).

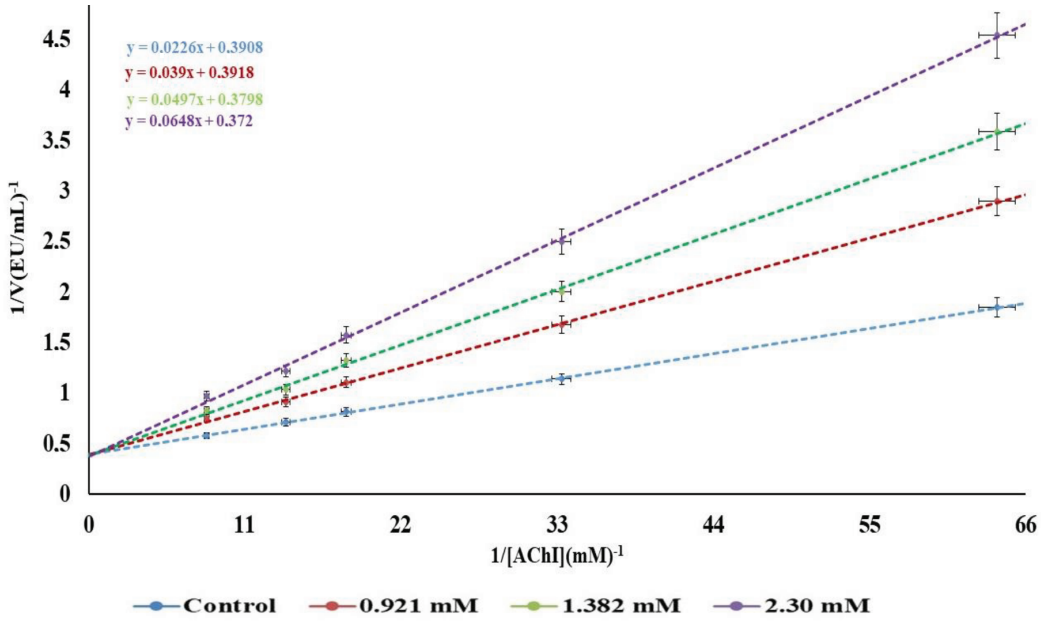

Figure 8. Effect of $[Ag(CN)_2(H_2O)K]$ on AChE enzyme inhibition (Lineweaver–Burk).

medium. Coordination polymers containing dicyanoargentate(I) have remarkable biological activities because of their therapeutic properties due to their pharmaceutical properties. Silver-bearing cyanide complex affects the inhibition of the enzyme that plays a role in biochemical reactions that are important for the quality of human life. In this study, we investigated AChE. As a result, the compound showed inhibition at the millimolar levels (1.32 mM, (r2: 0.99)) against the AChE enzyme. The compound was a good inhibitor for the AChE enzyme. This type of compound can therefore be used for the development of novel anticholinesterase drugs.

Table 4. Inhibition results of acetylcholinesterase (IC_{50} and Ki values).

Complex	*Enzymes*	*AChE (mM)*
	IC_{50}	1.32
	r^2	0.99956
	Ki+std	0.0282 ± 0.010
	Enzymes	AChE (μM)
Standard (tacrine for AChE)	IC_{50}	409.10
	r^2	0.9601
	Ki+std	392.18 ± 66.28

Acknowledgments

The author would like to thank the Bartın University Research Foundation (2019-Fen-B-004), O. Şahin from Sinop University for the X-ray analysis, and D. Kısa from the Department of Molecular Biology and Genetics, Faculty of Science, Bartın University for the enzymatic activity.

References

1. Stevens MP. In Polymer Chemistry: An Introduction. 3rd ed.. Oxford, UK: Oxford University, 1999, pp. 425-446.
2. Munakata M, Wu LP, Kuroda-Sowa T. Toward the construction of functional solid-state supramolecular metal complexes containing copper(I) and silver(I). Advances in Inorganic Chemistry 1999; 46: 173-303.
3. Wu HP, Janiak C, Rheinwald G, Lang H. 5,5′-Dicyano-2,2′-bipyridine silver complexes: discrete units or cordination polymers through a chelating and/or bridging metal–ligand interaction. Journal of the Chemical Society, Dalton Transactions 1999; 183-190.
4. Karadağ A. Preparation, spectra and thermal properties of two novel cyano-bridged complexes: crystal structure of one-dimensional copper(II)/palladium (II). Zeitschrift für Kristallographie 2007; 222: 39-45.
5. Karadağ A, Aslan Korkmaz Ş, Andaç Ö, Yerli Y, Topcu Y. Cyano-complexes and salts with tetracyanonickellate^{II} and N,N-bis(2-hydroxyethyl)-ethylenediamine: synthesis, IR spectra, magnetic properties, thermal analyses, and crystal structures. Journal of Coordination Chemistry 2012b; 65: 1685-1699.
6. Karadağ A, Bulut A, Şenocak A, Uçar İ, Büyükgüngör O. Preparations, IR spectra and crystal structures cyano-bridges bimetallic complexes of Zinc(II) and Cadmium(II) with tetracyanopalladate(II). Journal of Coordination Chemistry 2007; 60: 2035-2044.
7. Karadağ A, Önal İ, Şenocak A, Uçar İ, Bulut A et al. Syntheses, IR spectra, thermal properties and crystal structures of novel cyano-bridged polymeric complexes of zinc^{II} and cadmium^{II} with tetracyanoplatinate^{II}. Polyhedron 2008; 27: 223-231.
8. Karadağ A, Paşaoglu H, Kaştaş G, Büyükgüngör O. Polymeric μ-cyano-dicyanonickelate(II)-μ-cyano-trans-bis[N-(2-hydroxyethyl)ethylenediamine] cadmium (II). Acta Crystallographica 2004; C60: m581-m583.
9. Karadağ A, Paşaoglu H, Kaştaş G, Büyükgüngör O. Synthesis, IR spectrum, thermal behaviour and crystal structure of a novel one-dimensional cyano-bridged zinc(II)/nickel(II) complex. Zeitschrift für Kristallographie 2005; 220: 74-78.
10. Karadağ A, Şenocak A, Önal İ, Yerli Y, Şahin E et al. Preparation, structural, magnetic and thermal properties of two heterobimetallic cyano-bridged nickel(II)-copper(II)/platinum(II) coordination polymers. Inorganica Chimica Acta 2009; 362: 2299-2304.

11. Karadağ A, Şenocak A, Yerli Y, Şahih E, Topkaya R. Complexes containing N-(2-hydroxyethyl)-ethylenediamine with tetracyanometallate (II): synthesis, IR spectra, thermal behavior, crystal structure, magnetic properties and catalysis. Journal of Inorganic and Organometallic Polymers 2012a; 22: 369-378.
12. Karadağ A, Korkmaz N, Aydın A, Tekin Ş, Yanar Y et al. In vitro biological properties and predicted DNA–BSA interaction of three new dicyanidoargentate(I)-based complexes: synthesis and characterization. New Journal of Chemistry 2018; 42: 4679-4292.
13. Aydın A, Karadağ A, Tekin Ş, Korkmaz N, Özdemir A. Two new coordination polymers containing dicyanidoargentate(I) and dicyanidoaurate(I): Synthesis, characterization and a detailed investigation as in vitro of their anticancer activities on some cancer cell lines. Turkish Journal of Chemistry 2015; 39: 532-549.
14. Aydın A, Korkmaz N, Tekin Ş, Karadağ A. Anticancer activities and mechanism of action of two novel metal complexes, C16H34N8O5Ag2Cd and C11H16N7O2Ag3Ni. Turkish Journal of Biology 2014; 38: 948-955.
15. Isildak O, Saymaz F, Karadag A, Okumus Korkmaz N, Attar A. A novel potentiometric sensor for determination of neurotoxin β-N-oxalyl-L-α,β-diaminopropionic acid. BioMed Research International, 2014; 251653: 1-5.
16. Aslan Korkmaz Ş, Karadağ A, Korkmaz N, Andaç Ö, Gürbüz N et al. Five complexes containing N,N-bis(2-hydroxyethyl)-ethylenediamine with tetracyanidopalladate(II): Synthesis, crystal structures, thermal, magnetic and catalytic properties. Journal of Coordination Chemistry 2013; 66 (17): 3072-3091.
17. Abu-Youssef MAM, Langer V, Öhrström L. Synthesis, a case of isostructural packing, and antimicrobial activity of silver(I)quinoxaline nitrate, silver(I)(2,5-dimethylpyrazine) nitrate and two related silver aminopyridine compounds. Dalton Transactions 2006; 21: 2542-2550. doi: 10.1039/B516723J
18. Jaros SW, Da Silva MFCG, Król J, Oliveira MC, Smoleński P et al. Bioactive silver-organic networks assembled from 1,3,5-triaza-7-phosphaadamantane and flexible cyclohexanecarboxylate blocks. Inorganic Chemistry 2016; 55: 1486-1496. doi: 10.1021/acs.inorgchem.5b02235
19. Massoud AA, Langer V, Abu-Youssef MAM. Bis[4-(dimethylamino)pyridine-kappaN1]silver(I)nitrate dehydrate. Acta Crystallographica 2009; C65: m352-m354. doi: 10.1107/S0108270109030509
20. Abu-Youssef MAM, Soliman SM, Sharaf MM, Albering JH, Öhrström L. Topology analysis reveals supramolecular organisation of 96 large complex ions into one geometrical object. CrystEngComm 2016; 18: 1883-1886. doi: 10.1039/ C5CE02490K
21. Jaros SW, Da Silva MFCG, Florek M, Smoleński P, Pombeiro AJL et al. Silver(I) 1,3,5-triaza-7-phosphaadamantane coordination polymers driven by substituted glutarate and malonate building blocks: self-assembly synthesis, structural features, and antimicrobial properties. Inorganic Chemistry 2016; 55: 5886-5894. doi: 10.1021/acs. inorgchem.6b00186
22. Smoleński P, Jaros SW, Pettinari C, Lupidi G, Quassinti L et al. New water-soluble polypyridine silver(I) derivatives of 1,3,5-triaza-7-phosphaadamantane (PTA) with significant antimicrobial and antiproliferative activities. Dalton Transactions 2013; 42: 6572-6581. doi: 10.1039/c3dt33026e
23. Morones-Ramirez J, Winkler JA, Spina CS, Collins J. Silver enhances antibiotic activity against gram-negative bacteria. Journal of Translational Medicine 2013; 5: 190ra81. doi: 10.1126/scitranslmed.3006276
24. Grunkemeier GL, Jin R, Im K, Holubkov R, Kennard ED, Schaff HV. Time-related risk of the St. Jude Silzone heart valve. European Journal of Cardio-Thoracic Surgery 2006; 30: 20-27. doi: 10.1016/j.ejcts.2006.04.012
25. Rocha DP, Pinto GF, Ruggiero R, De Oliveira CA, Guerra W et al. Coordination of metals to antibiotics as a strategy to combat bacterial resistance. Química Nova 2011; 34: 111-118. doi: 10.1590/S0100-40422011000100022
26. Nazari ZE, Banoee M, Sepahi AA, Rafii F, Shahverdi AR. The combination effects of trivalent gold ions and gold nanoparticles with different antibiotics against resistant Pseudomonas aeruginosa. Gold Bull 2012; 45: 53-59. doi: 10.1007/ s13404-012-0048-7

27. Banti CN. Anti-proliferative and anti-tumor activity of silver(I) compounds. Metallomics 2013; 5: 569-596. doi: 10.1039/c3mt00046j

28. Korkmaz N, Ceylan Y, Karadağ A, Bülbül AS, Aftab MN et al. Biogenic silver nanoparticles synthesized from *Rhododendron ponticum* and their antibacterial, antibiofilm and cytotoxic activities, Journal of Pharmaceutical and Biomedical Analysis 2019; 112993: 1-8. doi: 10.1016/j.jpba.2019.112993

29. Korkmaz N. Bioreduction; The biological activity, characterization and synthesis of silver nanoparticles. Turkish Journal Of Chemistry 2020; 44: 325-334. doi: 10.3906/kim-1910-8

30. Korkmaz N, Karadağ A, Aydın A, Yanar Y, Karaman İ et al. Synthesis and characterization of two novel dicyanidoargentate complexes containing $N-$(2-hydroxyethyl)ethylenediamine exhibiting significant biological activity. New Journal of Chemistry 2014; 38(10): 4760-4773.

31. Korkmaz N, Aydın A, Karadağ A, Yanar Y, Maaşoğlu Y et al. New bimetallic dicyanidoargentate(I)-based coordination compounds: Synthesis, characterization, biological activities and DNA-BSA binding affinities. Spectrochimica Acta Part A: Molecular and Biomolecular Spectroscopy 2017; 173: 1007-1022.

32. Wen C, Yin A, Dai W. Recent advances in silver-based heterogeneous catalysts for green chemistry processes. Applied Catalysis B: Environmental 2014; 160: 730-741. doi: 10.1016/j.apcatb.2014.06.016

33. Lo VK, Chan AO, Che C. Gold and silver catalysis: from organic transformation to bioconjugation. Organic & Biomolecular Chemistry 2015; 13: 6667-6680. doi: 10.1039/C5OB00407A

34. Ellman GL, Courtney KD, Andres V, Featherston RM. A new and rapid colorimetric determination of acetylcholinesterase activity. Biochemical Pharmacology 1961; 7: 88e95.

35. Ono D, Bamba T, Oku Y, Yonetani T, Fukusaki E. Application of fourier transform near-infrared spectroscopy to optimization of green tea steaming process conditions. Journal of Bioscience and Bioengineering 2011; 112 (3): 247-251.

36. Lin SY, Wang SL. Advances in simultaneous DSC–FTIR microspectroscopy for rapid solid-state chemical stability studies: some dipeptide drugs as examples. Advanced Drug Delivery Reviews 2012; 64: 461-478.

37. Nakamoto K. Infrared and raman spectra of inorganic and coordination compounds. New York, NY, USA: Wiley Interscience Publication 2008, p. 484.

38. Venugopal A, Berger RJ, Willner A, Pape T, Mitzel KB. Potasyum hidroksilamin kompleksleri. Inorganic Chemistry 2008; 47 (11): 4506-4512.

39. Naktode K, Bhattacharjee J, Chakrabarti A, Panda TK. Syntheses and structures of dimeric sodium and potassium complexes of 2, 6-diisopropyl-anilidophosphine borane ligand. Journal of Chemical Sciences 2015; 127 (2): 265-272.

40. Langer J, Grams S, Puchta R. Lithium and potassium complexes with dbn- and dbu-based enamido phosphine ligands: Syntheses and applications. European Journal of Inorganic Chemistry 2017; 2017 (20): 2671-2681.

41. Gocer H, Topal F, Topal M, Küçük M, Teke D et al. Acetylcholinesterase and carbonic anhydrase isoenzymes I and II inhibition profiles of taxifolin. Journal of Enzyme Inhibition and Medicinal Chemistry 2016; 31 (3): 441-447.

42. Pietsch M, Christian L, Inhester T, Petzold S, Gütschow M. Kinetics of inhibition of acetylcholinesterase in the presence of acetonitrile. The FEBS Journal 2009; 276 (8): 2292-2307.

43. Taslimi P, Caglayan C, Farzaliyev V, Nabiyev O, Sujayev A et al. Synthesis and discovery of potent carbonic anhydrase, acetylcholinesterase, butyrylcholinesterase, and ??-glycosidase enzymes inhibitors: Thenovel $N, N\prime-$ biscyanomethylamine and alkoxymethylamine derivatives. Journal of Biochemical and Molecular Toxicology 2018; 32 (4): e22042.